THE JOURNAL OF BIOLOGICAL CHEMISTRY
Vol. 273, No. 14, Issue of April 3, pp. 7856–7864, 1998

Printed in U.S.A.

Connexin Membrane Protein Biosynthesis Is Influenced by Polypeptide Positioning within the Translocon and Signal Peptidase Access*

(Received for publication, November 3, 1997, and in revised form, January 27, 1998)

Matthias M. Falk‡ and Norton B. Gilula

From the Department of Cell Biology, The Scripps Research Institute, La Jolla, California 92037

We reported previously (Falk, M. M., Kumar, N. M., and Gilula, N. B. (1994) *J. Cell Biol.* 127, 343–355) that the membrane integration of polytopic connexin polypeptides can be accompanied by an inappropriate cleavage that generates amino-terminal truncated connexins. While this cleavage was not detected *in vivo*, translation in standard cell-free translation/translocation systems resulted in the complete cleavage of all newly integrated connexins. Partial cleavage occurred in heterologous expression systems that correlated with the expression level. Here we report that the transmembrane topology of connexins generated in microsomal membranes was identical to the topology of functional connexins in plasma membranes. Characterization of the cleavage site and reaction showed that the connexins were processed by signal peptidase immediately downstream of their first transmembrane domain in a reaction similar to the removal of signal peptides from pre-proteins. Increasing the length and hydrophobic character of the signal anchor sequence of connexins completely prevented the aberrant cleavage. This result indicates that their signal anchor sequence was falsely recognized and positioned as a cleavable signal peptide within the endoplasmic reticulum translocon, and that this mispositioning enabled signal peptidase to access the cleavage sites. The results provide direct evidence for the involvement of unknown cellular factors in the membrane integration process of connexins.

Translocation of membrane proteins is a complex process. It involves recognition and targeting of the proteins to the endoplasmic reticulum (ER)[1] membrane, their insertion into the lipid bilayer with their correct transmembrane (TM) orientation without interrupting the permeability barrier of the membrane bilayer, and finally, their maturation into functional proteins that includes co- and post-translational processes such as signal peptidase (SPase) cleavage of ER target signal sequences, folding, disulfide bridge formation, glycosylation, and other post-translational modifications, and eventually oligomerization. A large portion of the current knowledge on the synthesis and translocation of secretory and membrane proteins has been obtained by synthesizing these proteins in translation competent cell lysates supplemented with ER-derived membrane vesicles (microsomes) (1). Since the lysate system has been found in many cases to accurately reproduce the steps involved in translation, translocation, and co- and post-translational modifications, it has become a standard assay system to study these processes. Many secretory and predominantly single spanning TM proteins have been investigated using this assay system, and a large body of information on the mechanisms involved in the membrane translocation of these protein types has been accumulated (reviewed in Refs. 2–4). However, little is known about the synthesis of polytopic membrane proteins that traverse the membrane bilayer more than once. This holds true in particular for membrane channel proteins that bear charged amino acid residues within their TM domains to allow the formation of a hydrophilic pore within the membrane bilayer. Experimental evidence indicates that secretory, as well as TM proteins use the same translocation machinery, and that many of the steps that are involved in the biogenesis of both protein types are closely related (3, 5, 6). However, several recent discoveries indicate that the current understanding of membrane protein translocation is quite incomplete, and it may be much more versatile than previously expected (reviewed in Ref. 4).

We used connexin (Cx) polypeptides as model proteins to study the steps involved in the synthesis of channel forming membrane proteins. Cxs are the proteins that form gap junctions, TM channels providing direct cell-to-cell communication. They are nonglycosylated, polytopic plasma membrane (PM) proteins (class III membrane proteins) that traverse the membrane bilayer four times with NH_2 and COOH termini located in the cytoplasm (N_{cyt}-C_{cyt} orientation). This TM topology was suggested by hydropathy analyses of the primary amino acid sequences and is supported by many other topological analyses (cited in Ref. 7). More than a dozen different Cxs have been cloned and sequenced from rodents, and all represent structurally conserved members of a multigene family that mainly differ in the length of their COOH-terminal domains. To form a gap junction channel, 6 Cxs oligomerize into a ring-shaped structure with a central hydrophilic pore, termed connexon. Two connexons, each provided by two neighboring cells then pair in the adjacent PMs to form the transcellular, double-membrane channel (reviewed in Refs. 8 and 9).

We found that the translation of Cx polypeptides in standard cell-free translation/translocation systems supplemented with ER-derived microsomes resulted in a complete, but inappropriate proteolytic processing that affected all Cx polypeptides upon their membrane integration (reported in this study and in

* This research was supported by National Institutes of Health Grant GM 37904, a grant from the Lucille P. Markey Charitable Trust (to N. B. G.), and a Deutsche Forschungsgemeinschaft fellowship (to M. M. F.). The costs of publication of this article were defrayed in part by the payment of page charges. This article must therefore be hereby marked "*advertisement*" in accordance with 18 U.S.C. Section 1734 solely to indicate this fact.

‡ To whom all correspondence should be addressed: Dept. of Cell Biology, MB6, The Scripps Research Institute, 10550 North Torrey Pines Rd., La Jolla, CA 92037. Tel.: 1-619-784-2352; Fax: 1-619-784-2345; E-mail: MFalk@scripps.edu.

[1] The abbreviations used are: ER, endoplasmic reticulum; Cx, connexin; PM, plasma membrane; SA, signal anchor; PAGE, polyacrylamide gel electrophoresis; SP, signal peptide; SPase, signal peptidase; TM, transmembrane; wt, wild type; CAPS, 3-(cyclohexylamino)-1-propanesulfonic acid; CHES, 2-(*N*-cyclohexylamino)ethanesulfonic acid; NEM, *N*-ethylmaleimide; PL, prolactin.

Ref. 7). Functional Cxs organized in gap junction plaques at the PM are not processed in this manner (10, 11). This difference in Cx membrane integration *in vitro* and *in vivo* suggested that the membrane integration process of Cxs somehow differs from the membrane integration of previously studied membrane proteins and may require additional factors which are absent in the cell-free translation system. Further analysis showed that a comparable cleavage product was also detectable in the ER membranes of different cell types that overexpress Cxs. There, the amount of cleaved Cx polypeptides correlated with the expression level (7). The cleavage reaction clipped off an NH_2-terminal portion of the Cx polypeptides, and appeared to be similar to the cleavage of target signal peptides (SP) from pre-proteins synthesized on the ER membrane. Further characterization indeed suggested a cleavage by SPase (12), the enzyme that normally cleaves NH_2-terminal ER target SPs from secretory and certain TM pre-proteins oriented with their NH_2 terminus located in the lumen of the ER. Cxs, however, are oriented with their NH_2 terminus facing the cytoplasm, and no NH_2-terminal SP is encoded within their NH_2 terminus. Instead, internal hydrophobic signal anchor (SA) sequences have been characterized in N_{cyt}-oriented membrane proteins, such as the Cxs, that function in their membrane targeting and anchoring (reviewed in Refs. 2–4). Consequently, Cxs should not be cleaved by this enzyme upon their membrane integration.

Here we report the TM topology of Cxs generated in ER membranes, and that a modified TM orientation is not causing this inappropriate cleavage. Furthermore, we performed an extensive characterization of the cleavage site, reaction, and conditions that are associated with this proteolytic processing. The results indicated that the SA sequence of Cxs was improperly recognized and positioned within the ER translocon when Cxs were translocated *in vitro*, and that this mis-positioning allowed SPase to access the cleavage sites in the Cx sequences. The results provide direct evidence that additional, unknown cellular factors are involved in the successful membrane integration of Cx polypeptides *in vivo* that are absent or not functional in standard cell-free translation/translocation systems.

EXPERIMENTAL PROCEDURES

cDNA Clones, Chimeras, and Mutagenesis of Cx Polypeptides—For the *in vitro* transcription of efficiently translated synthetic Cx RNAs, rat α_1 (Cx43), and human β_1 (Cx32) cDNAs were cloned into the transcription vector pSP64T (13) as described in Falk *et al*. (7).

Site-directed mutagenesis of the Cx sequences was performed using overlap extension polymerase chain reaction as described in Falk *et al*. (14), except that proofreading PFU polymerase (Stratagene, La Jolla, CA) was used. Plasmids pSP64Tα_1 and β_1 were cut with *Nhe*I, dephosphorylated, and the wt sequences were replaced with the *Nhe*I-cut polymerase chain reaction amplified mutagenic cDNA fragments. For rapid identification of mutated clones, nucleotide exchanges were chosen that, in addition to the desired amino acid substitution, created new endonuclease restriction sites. Clones with correctly oriented inserts were determined by restriction endonuclease mapping, and selected constructs were verified by DNA sequencing.

N-Glycosylation consensus sites with the general amino acid sequence NXS or NXT (15) were introduced into the β_1 Cx sequence by substituting specific amino acid residues in different Cx domains supposed to be located on either side of the membrane bilayer. Selected amino acid residues around the SPase cleavage sites determined in α_1 Cx and in β_1 Cx were substituted in the α_1 Cx sequence. Double α1 Cx mutants having both α1 and β_1 Cx cleavage sites mutated were created by using the respective single site mutants as template DNAs. β_1 Cx mutants with an increased hydrophobic character of the first transmembrane domain (TM1) were created by exchanging the central arginine (Arg-32) residue in the hydrophobic (h) core region of TM1 with leucine (Leu), and/or three additional leucine codons were inserted immediately downstream of the Arg-32 codon into the TM1 domain.

A Bluescript-based plasmid containing the wild type synaptophysin cDNA was generously provided by R. Scheller (Howard Hughes Medical Institute, Stanford, CA). To increase *in vitro* translation efficiency, the synaptophysin cDNA was recloned into the *in vitro* transcription vector pSP64T (13). Bluescript KS-based plasmids pCSR2, pCSR3, pCSR4, and pCSR5, encoding β_1 Cx/synaptophysin chimeras, in which the Cx sequence is progressively replaced by synaptophysin sequence, were generously provided by R. Leube (University of Mainz, Mainz, Germany). Construction of the chimeras is described in Leube (16). The pSP64T-based plasmid pBP4 encoding bovine preprolactin was kindly provided by D. Zopf and P. Walter (University of California, San Francisco, CA). A pSP64T-based plasmid encoding rat lens membrane protein MP26 was kindly provided by N. M. Kumar (The Scripps Research Institute, La Jolla, CA).

In Vitro Transcription, Translation, and Membrane Translocation Assay—All plasmids used for *in vitro* transcription were linearized, phenol/chloroform extracted, and ethanol precipitated prior to RNA synthesis. Transcription reactions were performed using T3, T7, or SP6 RNA polymerase (Promega Biotech, Madison, WI). The quality and amount of synthesized RNA was determined by analyzing aliquots on agarose gels. Synthetic RNAs were either used immediately or stored in aliquots at −70 °C.

Cell-free translation reactions were performed as described previously (7, 17). Nuclease-treated rabbit reticulocyte lysates were purchased from Promega Biotech and programmed with synthetic RNA. Typically 0.5–1 μg of RNA was used per 25-μl reaction volume. RNAs were translated in the presence of L-[^{35}S]methionine (555 MBq/ml, Amersham Corp.). Translation reactions were supplemented co-translationally with canine pancreas-derived rough microsomes, which were either obtained from Promega Biotech or prepared as described by Walter and Blobel (18). Typical concentrations were 0.5–1 Eq/10-μl reaction volume (18). Translation reactions were incubated at 30–35 °C for 30–60 min except as otherwise stated. Membrane bound proteins were harvested by pelleting the microsomes through a 0.5 M sucrose cushion, using an Airfuge ultracentrifuge (Beckman Instruments, Inc., Palo Alto, CA), as described in Falk *et al.* (7). To remove *N*-linked carbohydrates from the *N*-glycosylated Cx constructs, 10-μl aliquots of the corresponding translocation reactions were incubated with 1 unit of endoglycosidase H (Boehringer Mannheim) for 2 h at room temperature prior to immunoprecipitation. To test a possible influence of the pH on the cleavage reaction, increasing volumes of 50 mM NaCl or NaOH solutions were added to the translocation reactions.

Pretreatment of Microsomal Vesicles—Microsomal vesicles were depleted of their lumenal proteins by perforating them at high pH as described (19), except that CAPS (pK_a 10.4) was replaced with CHES (pK_a 9.3). 100-μl microsome aliquots were diluted 10-fold with either 50 mM (final concentration) HEPES buffer (pK_a 7.55), pH 7.4, or 50 mM (final concentration) CHES buffer, pH 9.5 and pH 10.2, and incubated on ice for 30 min. Microsomes were neutralized and collected as described (19), and stored on ice until used. Depletion of their soluble, lumenal proteins was monitored by analyzing the protein content in the supernatants on Coomassie Blue-stained SDS-PAGE gels. To ensure protease inhibitor access to the lumen, microsomes were perforated as described above and preloaded with *N*-ethylmaleimide (NEM; 0.25 and 1 mM final concentration), iodoacetamide (1 mM final concentration), EDTA (1 mM final concentration), EGTA (2 mM final concentration), or diisopropyl fluorophosphate (2 mM final concentration) (Sigma) by adding these inhibitors to the perforation buffers.

Radiosequencing of α_1 and β_1 Cx—For radiosequencing, Cxs were labeled with L-[2,3,4,5,6-^{3}H]phenylalanine (37 MBq/ml, Amersham Corp.). A complete amino acid mixture (1 mM final concentration) lacking phenylalanine (Phe) was prepared from amino acid calibration markers (Sigma). A standard translation reaction (60 μl) consisted of 30 μl of reticulocyte lysate, 3 μl of 1 mM amino acid mixture without Phe, 15 μl of [^{3}H]Phe, 1–3 μg of synthetic RNA, and 6–8 equivalents of microsomes. After translation the reaction was loaded on SDS-PAGE gels, and the areas containing the α_1 or β_1 Cx polypeptides were excised, cut into smaller pieces, and placed into the chamber of an ELUTRAP elution device (Schleicher & Schuell, Keene, NH). The elution buffer (0.1% SDS, 20 mM NH_4HCO_3, 1 mM thioglycolic acid, 0.1% dithiothreitol) was continuously mixed by pumping the buffer from the negative pole to the positive pole with a peristaltic pump (Bio-Rad). Proteins were eluted overnight at 100 V. The eluate (~1 ml/chamber) was dried and SDS removed by ion-pair extraction with unhydrous acetone/triethylamine/acetic acid/water (85:5:5:5). Cxs were then solubilized in 0.1% SDS solution and protein corresponding to ~100,000–200,000 cpm were applied to a Polybrene-treated glass fiber filter for 20–25 cycles of amino acid sequence analysis in an Applied Biosystems 470A gas-phase sequenator (Foster City, CA). Individual cycles were collected before on-line high performance liquid chromatography analysis. 50-μl

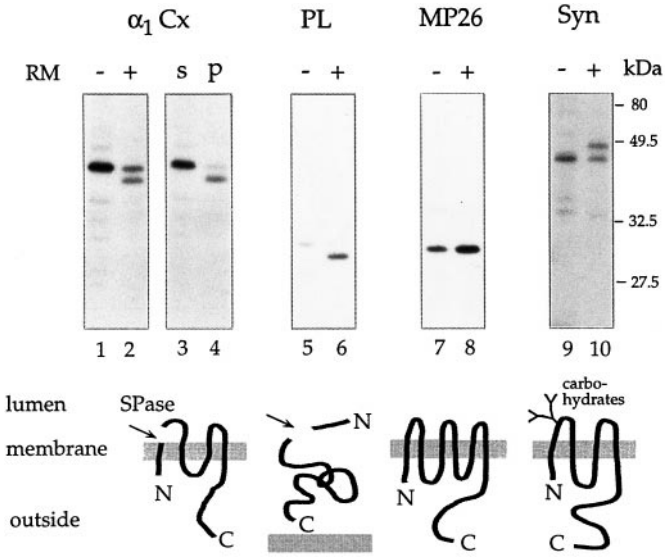

FIG. 1. **Cell-free integration of Cxs and other secretory and membrane proteins into microsomal membranes.** α_1 Cx (*lanes 1* and *2*), PL (*lanes 5* and *6*), MP26 (*lanes 7* and *8*), and Syn (*lanes 9* and *10*) were translated in reticulocyte lysates programmed with the respective synthetic RNAs in the absence (−) and presence (+) of microsomes. [^{35}S]Methionine-labeled translation products were analyzed by SDS-PAGE and visualized by autoradiography. α_1 Cx translocation reactions were separated into membrane integrated (*p*), and non-membrane integrated polypeptides (*s*) by pelleting the microsomes through sucrose cushions (*lanes 3* and *4*). Faster migrating, aberrantly cleaved Cx translation products were generated in the presence of microsomes. Predicted translation products were obtained with secretory (PL) and other membrane protein RNAs (MP26 and Syn) that were translated in parallel reactions. Corresponding topology schemes including the respective co- and post-translational modifications are shown. The position of molecular mass protein standards (in kDa) are indicated on the *right* in Figs. 1, 2, and 6.

aliquots were mixed with scintillation mixture (Bio-Safe II, Research Products International Corp., Mount Prospect, IL) and analyzed by liquid scintillation counting. Radioactive peak activities were aligned with phenylalanine residues in the Cx sequence to determine the exact position of the cleavage site.

Gel Electrophoresis, Autoradiography, and Densitometry—Translation products were analyzed on 10 and 12.5% SDS Laemmli gels (acrylamide/bisacrylamide ratio, 29:1). Samples were solubilized in SDS sample buffer containing 3% SDS, 5% β-mercaptoethanol, and analyzed without heating to prevent aggregation of Cx polypeptides. Following electrophoresis, gels were soaked for 10 min in 1 M sodium salicylate (Sigma) to enhance ^{35}S and ^{3}H-autoradiography, dried, and exposed to Kodak X-AR film at −70 °C using an intensifying screen. To determine cleavage efficiency of the SPase cleavage site mutants, autoradiographs were scanned densitometrically using an AlphaImager 2000 Digital Imaging and Analysis System (Alpha Innotech Corp., San Leandro, CA). Average cleavage efficiencies of the mutants were expressed in percent compared with the cleavage efficiency of wild type α_1 Cx.

RESULTS

Cell-free Expression of Cxs—For the analysis of the Cx biogenesis described in this study, the two most abundant Cx isotypes, heart Cx α_1 (Cx43) and liver Cx β_1 (Cx32), were used. As we reported previously, Cx polypeptides can be expressed efficiently as full-length proteins in reticulocyte lysates or wheat germ extracts in the absence of microsomes. Synthetic Cx RNAs produced translation products that migrated with an electrophoretic mobility on SDS-PAGE gels that corresponded to their predicted molecular weights (Fig. 1, *lane 1*, shown for α_1 Cx; see also Ref. 7). However, translation in the presence of pancreatic microsomes resulted in the generation of cleaved Cxs with a faster mobility on SDS-PAGE gels (Fig. 1, *lane 2*) that were retained in the microsomal membrane fraction after pelleting the microsomes through a 0.5 M sucrose cushion (Fig. 1, *lanes 3* and *4*). All Cx isotypes examined thus far were aberrantly processed in this manner (7). Full-length Cx polypeptides also generated in the presence of microsomes (Fig. 1, *lane 2*) were not membrane associated and stayed in the supernatant fraction (Fig. 1, *lane 3*), indicating that they were synthesized by free ribosomes that failed to bind to the membranes. Other secretory and transmembrane proteins, such as prolactin (PL), MP26, and synaptophysin (Syn), translated in parallel reactions in the presence of microsomes gave results as reported previously, namely SP cleavage of pre-prolactin (20), membrane integration of MP26 without SP cleavage or glycosylation (21), and membrane integration and *N*-glycosylation of Syn (22), respectively (Fig. 1, *lanes 5–10*).

The TM Topology of Cxs Integrated into ER Membranes Was Identical to Their Topology in the PM—The TM topology of Cxs integrated into microsomes was determined by *N*-glycosylation site tagging. *N*-Glycosylation consensus sequences were introduced into the extracellular loops (E1 and E2), and into the intracellular loop (I-loop) described to be located on both sides of the PM (Fig. 2*A*). While the β_1 mutants with the consensus sites in the extracellular loop E1 (designated β_1E1K48N and β_1E1L56S), or E2 (designated β_1E2L165N/K167S) were efficiently glycosylated resulting in a reduced mobility on SDS-PAGE gels (Fig. 2*B, lanes 5, 8,* and *14*), the mutant with the consensus site in the I-loop (designated β_1I-loopH126N) was not glycosylated (Fig. 2*B, lane 11*). Endoglycosidase H (endoH) digestion removed the carbohydrate side chains and shifted their electrophoretic mobility back to the mobility of the wt protein (Fig. 2*B, lanes 6, 9*, and *15*). Protease protection assays have shown previously that the COOH-terminal domain of the Cxs is located correctly outside the microsomes (7). Taken together, these results demonstrated that the TM topology of Cx polypeptides integrated into ER membranes (microsomes) was identical to their topology in the PM, and therefore, a hypothetical aberrant TM topology could not be responsible for the cleavage.

Polypeptide Translocation Was Required for Cx Cleavage—To determine whether Cx polypeptides have to be translocated into the lumen of the microsomes to be cleaved, we translated Cxs in the presence of microsomes that were preincubated with 0.25 and 1 mM NEM. This alkylating agent was previously reported to prevent protein translocation (23). To verify inhibition of protein translocation by NEM, Syn and PL were translated in parallel as control proteins. 0.25 mM NEM allowed the translocation of a portion of the control proteins, as indicated by a reduction in glycosylation of Syn, and a reduction of cleavage of pre-PL into PL. 1 mM NEM, however, completely abolished glycosylation of Syn, as well as cleavage of pre-PL, respectively (Fig. 3, *lanes 1–3, middle* and *bottom panels*). Successful targeting and binding of the newly translated polypeptides to the membrane was indicated by their recovery with the membranes after pelleting the microsomes through a 0.5 M sucrose cushion. Cx cleavage was completely abolished under the conditions described above (Fig. 3, *lanes 1–3, top panel*), indicating that membrane targeting was not sufficient for the Cx processing, but requires the translocation of the nascent Cx polypeptides into the membrane bilayer and into the lumen of the microsomes. Translocation and cleavage was also abolished when microsomes were preincubated at 30 °C for 30–90 min. This treatment resulted in the complete inactivation of the microsomal translocation activity (Fig. 3, *lanes 5–7*).

Cxs Were Aberrantly Cleaved by SPase upon Integration into Microsomes—A direct inhibitor for eucaryotic signal peptidases is not known, however, indirect experimentation reported in Falk *et al.* (7) suggested a cleavage by SPase. To obtain additional evidence for a SPase-mediated cleavage, microsomes

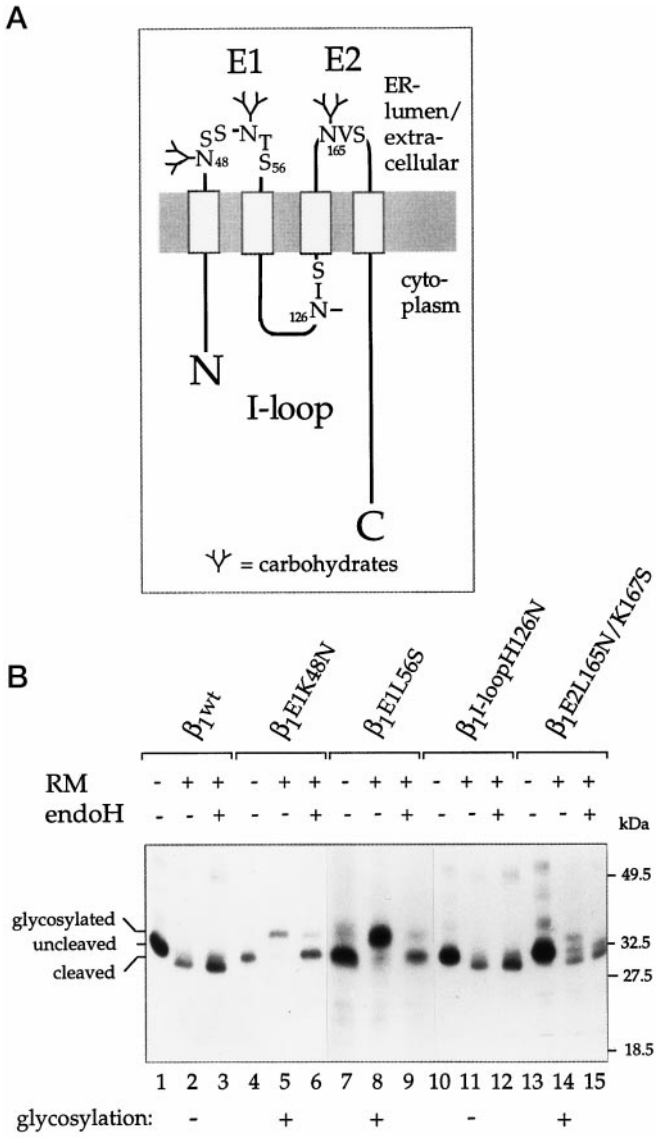

FIG. 2. **Analysis of the Cx transmembrane topology.** *A*, a topology scheme for β_1 Cx indicating the location and amino acid sequence of the *N*-glycosylation consensus sites that were introduced into different domains expected to be located on both sides of the membrane bilayer is shown. *B,* autoradiograms of the translation products obtained in the absence (−) and presence (+) of microsomes, and after digestion with endoglycosidase H (*endoH*) are shown. While mutants with the consensus sites in the extracellular loops (*E1* and *E2*) were efficiently glycosylated (*lanes 5, 8,* and *14*), resulting in a reduced mobility on SDS-PAGE gels, wild type β_1 Cx, as well as the mutant with the consensus site in the intracytoplasmic loop (I-loop) was not glycosylated (*lanes 2* and *11*). EndoH digestion removed the added carbohydrates and shifted the molecular weight back to the molecular weight of full-length Cxs (*lanes 6, 9*, and *15*).

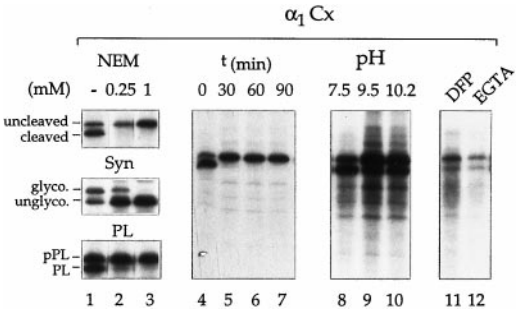

FIG. 3. **Characterization of the Cx cleavage reaction.** α_1 Cx translations were performed with microsomes pretreated with various conditions to determine the circumstances associated with the inappropriate cleavage of Cxs during microsomal membrane integration. Autoradiograms of the translation products analyzed by SDS-PAGE are shown. To inhibit protein translocation, microsomal vesicles were pretreated with NEM (*lanes 1–3*), or preincubated at 37 °C (*lanes 4–7*). Microsomes were depleted of lumenal soluble proteins by alkali treatment (*lanes 8–10*). Microsomes were preloaded with specific protease inhibitors (diisopropyl fluorophosphate (*DFP*) and EGTA) that block the known ER lumenal proteases, except SPase (*lanes 11* and *12*). Syn and PL were translated in parallel as controls to verify inhibition of translocation in the presence of NEM (*lanes 1–3, middle* and *bottom panels*).

were depleted of their soluble lumenal proteins by preincubating them at high pH (pH 9.5 and 10.2), using the protocol of Nicchitta and Blobel (19), followed by centrifugation through a 0.5 M sucrose cushion. However, protein depletion had little effect on the cleavage reaction (Fig. 3, *lanes 8–10*), indicating that the Cxs were not cleaved by a soluble, ER lumenal protease. Note that non-membrane integrated full-length Cxs generated as a by-product in the presence of microsomes (described above) were not removed prior to analysis, and therefore, are present on the gels shown in Fig. 3, *lanes 8–12*, and Figs. 5–7.

To exclude the possibility that the Cxs were cleaved by a different membrane-anchored ER protease, Cxs were translocated into microsomes that were preloaded at high pH with different class-specific protease inhibitors to ensure access of the chemicals to the microsomal lumen. While alkylating agents such as iodoacetamide (1 mM final concentration), or chelating agents such as EDTA (1 mM final concentration) efficiently blocked protein translation under the conditions described, preincubation of the microsomes in diisopropyl fluorophosphate (2 mM final concentration) or EGTA (2 mM final concentration), allowed translation, but had no significant influence on the cleavage reaction (Fig. 3, *lanes 11* and *12*). Furthermore, the cleavage was relatively independent of pH (~pH 5.5–9.0), temperature (30–41 °C), and RNA concentration (0.05–1 μg/10-μl reaction volume) (not shown). All these results provided additional strong evidence for a cleavage performed by SPase, and argued against a cleavage by any other known protease involved in protein degradation, such as "rapid ER degradation" (24) or "quality control" (25, 26).

Cxs Were Cleaved at SPase "Cleavage Site Motifs" in Their First Extracellular Domain—The exact location of the cleavage sites was mapped for cell-free expressed α_1 and β_1 Cx polypeptides by NH_2-terminal amino acid radiosequencing after translating the Cxs in the presence of labeled phenylalanine (Fig. 4*A*). Phenylalanine was chosen because of its unique distribution within the NH_2-terminal portion of the Cx polypeptide. While no Phe residues are present in the NH_2-terminal domain, two Phe residues separated by an isoleucine (Ile) are present in the first TM domain (Phe-29 and Phe-31 in β_1 Cx, and Phe-30 and Phe-32 in α_1 Cx). Finally, single or double Phe residues are present in the first extracellular loop (E1) (Phe-51 and Phe-68/Phe-69 in β_1 Cx, and Phe-52 and Phe-70 in α_1 Cx; Fig. 4*B*). Radioactive peak activities released in the individual degradation cycles (cycle 11 in the β_1 Cx and cycle 6 in the α_1 Cx sequencing reaction) best matched the distribution of Phe residues in the Cx sequences when aligned with Phe-51 of β_1 Cx and Phe-52 of α_1 Cx, respectively (Fig. 4, *A* and *B*). This analysis identified two cleavage sites separated by five amino acid residues from each other. Both sites were located within the border region between TM1 and E1, between alanine (Ala) 40 and glutamic acid (Glu) 41 in β_1 Cx, and glycine (Gly) 46 and aspartic acid (Asp) 47 in α_1 Cx, respectively (Fig. 4*A*). Both cleavage sites are homologous to natural SPase cleavage site motifs, small, uncharged amino acid residues in positions −3 and −1 with respect to the cleavage site (27), which are conserved in all Cx isotypes at these positions (see Fig. 4*B*).

The correct location of the cleavage site was confirmed by a

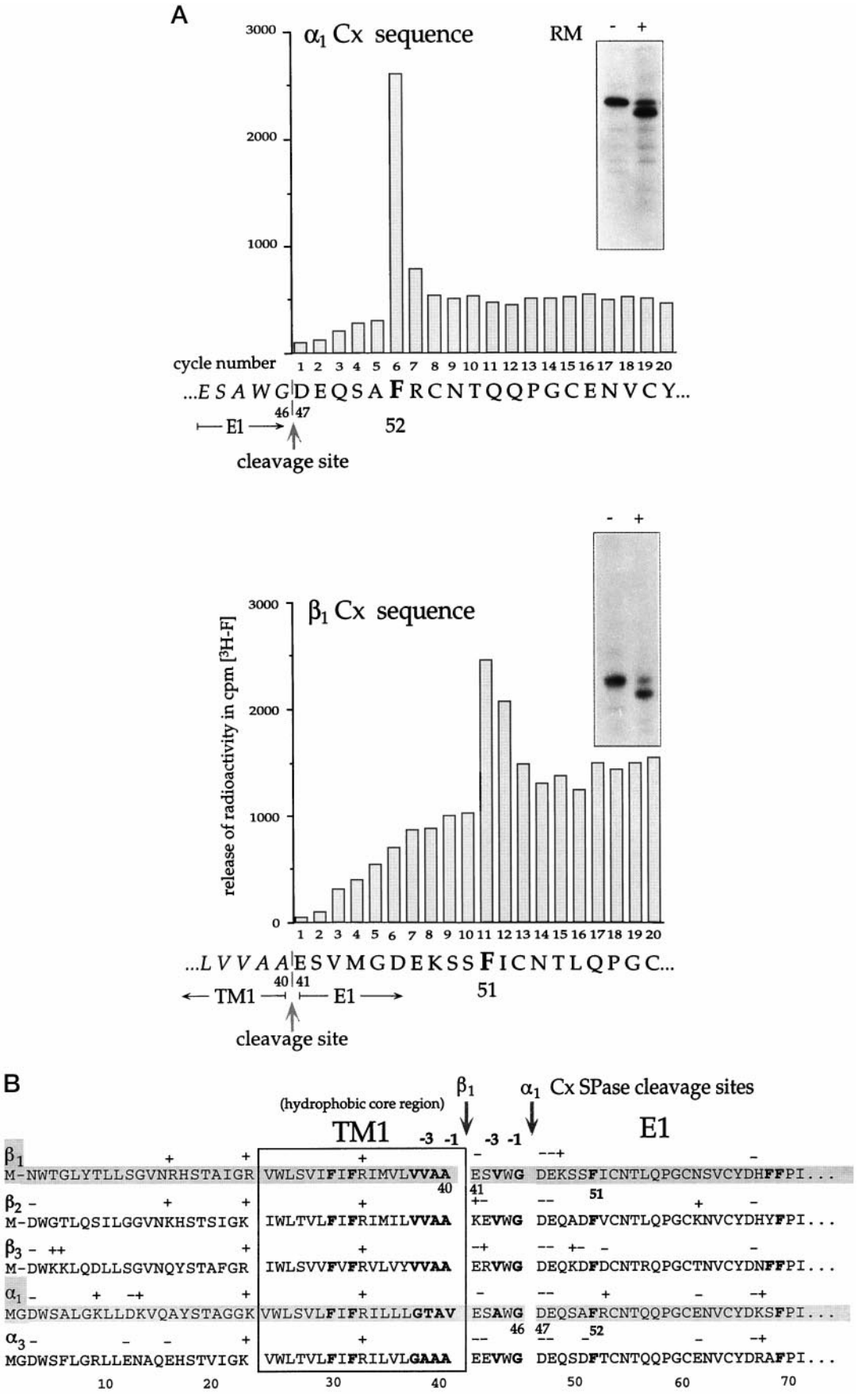

FIG. 4. **Determination of the cleavage site in Cxs.** *A*, the precise location of the cleavage sites was determined in cell-free integrated [^{3}H]phenylalanine-labeled, α_1 and β_1 Cx (lower protein bands generated in the presence of microsomes (+) shown on the gel insets) by sequential NH_2-terminal amino acid radiosequencing. In β_1 Cx the peak activity was obtained in cycle 11 that best matched the phenylalanine (F) distribution when aligned with Phe-51, identifying the cleavage site between alanine 40 (*A*) and glutamic acid 41 (*E*). In α_1 Cx the peak activity

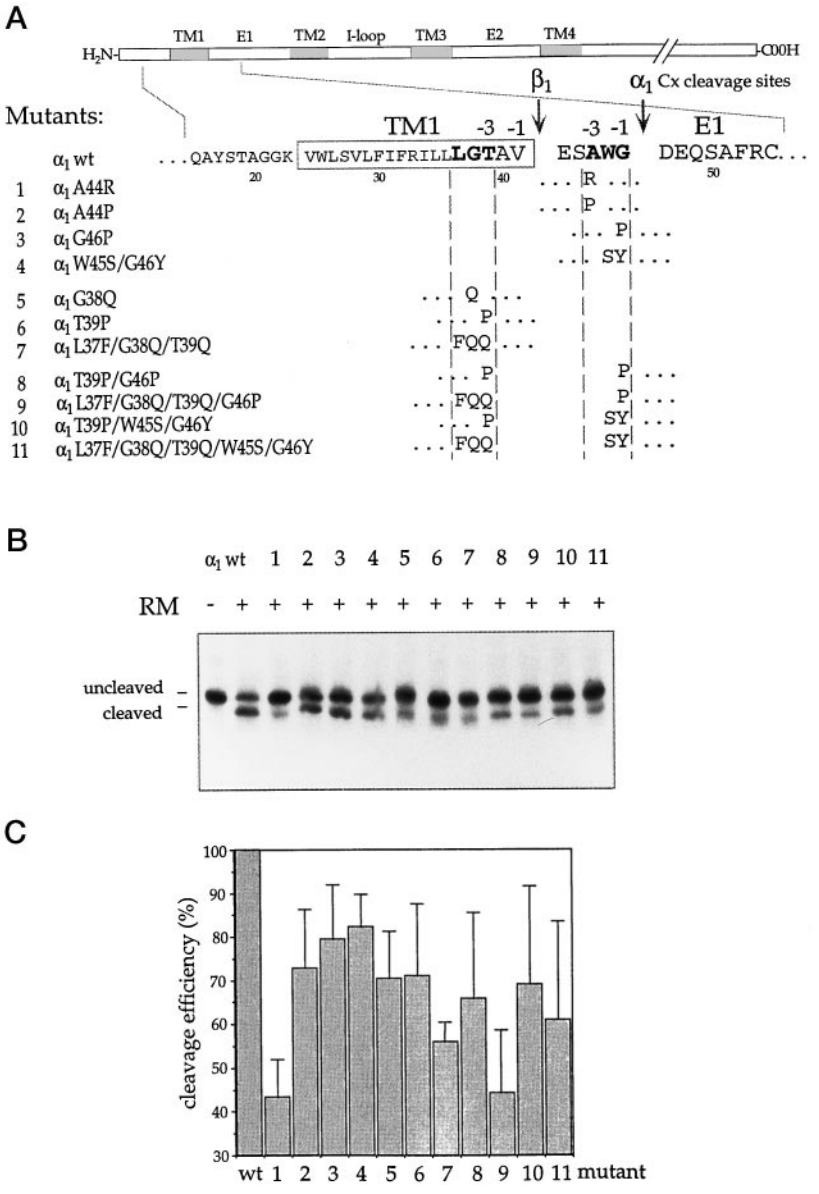

FIG. 5. **Mutational analysis of the cleavage site.** *A*, specific amino acid residues adjacent to the cleavage sites determined in α_1 and β_1 Cx were substituted in the α_1 Cx sequence with aromatic (*F* and *Y*), charged (*R*), large polar (*Q*), or proline (*P*) residues (mutants 1–11) which are not present at these positions in naturally SPase processed secretory and TM precursor proteins. A schematic representation of the α_1 Cx protein, including the location and amino acid sequence adjacent to the determined SPase cleavage sites are shown above. *B,* translation products obtained in the presence of microsomes (+) were analyzed by SDS-PAGE and autoradiography. *C,* cleavage efficiency (in %) was determined for each mutant by densitometric comparison of the amount of full-length *versus* cleaved polypeptides that were integrated into the microsomes.

site-directed amino acid substitution approach in the α_1 Cx sequence. Specific amino acid residues located within the −3/−1 motif identified in the α_1 Cx sequence (Fig. 5*A, mutants 1–4*), the β_1 Cx sequence (Fig. 5*A, mutants 5–7*), or within both cleavage site motifs (Fig. 5*A, mutants 8–11*), were exchanged with aromatic (Phe and Tyr), charged (Arg), large polar (Gln), or proline (Pro) residues. Residues with these characteristics are normally not present at these positions in wt precursor proteins naturally processed by SPase (27). Amino acid residue substitutions reduced proteolytic processing by 17.8–62.2% when compared with the processing efficiency of the wt α_1 Cx (Fig. 5*B* and *C, lanes 2–11*). However, none of the amino acid substitutions inhibited the cleavage reaction completely, indicating that either the mutants were processed at an alternative site (additional −3/−1 motifs are present in the proximity of the determined cleavage sites in the Cxs; see Fig. 4*B*), and/or that the introduced amino acid residues were only reducing, but not completely inactivating SPase cleavage activity.

The TM1 Domain and First Extracellular Loop (E1) Were Essential for Cx Polypeptide Processing—To determine which portion of the Cx polypeptides contains the information that enables SPase to access the cleavage sites, translation products of chimeric β_1 Cx/Syn proteins (designated pCSR2 to pCSR5 in Fig. 6) (16) were analyzed after their translation in the presence of microsomes. Syn is another tetra-spanning membrane protein with an N_{cyt}-C_{cyt} orientation with many similarities to the Cxs (22). In the chimeras, the Cx sequence (shown in *gray* in Fig. 6) was progressively replaced from the COOH terminus by Syn sequence (shown in *black* in Fig. 6). Replacing COOH-terminal portions of the Cx sequence did not prevent the cleavage (pCSR2 and pCSR3; Fig. 6, *lanes 4* and *6*), similar to the wt β_1 Cx protein (Fig. 6, *lane 2*). However, further replacing the

was obtained in cycle 6 that best matched the phenylalanine distribution when aligned with Phe-52, identifying the cleavage site between glycine 46 (*G*) and aspartic acid 47 (*D*). *B,* amino acid sequence alignment of the NH_2-terminal, TM1, and E1 domains of five different Cx isotypes, including α_1 and β_1 Cx (*underlayed* in *gray*). The cleavage sites determined in α_1 and β_1 Cx are indicated by *arrows*. The hydrophobic core region of TM1 (18 amino acid residues interrupted by a central arginine (*R*)) is *boxed*. Charged amino acid residues are marked with + and −. Phenylalanine residues (*F*) and small, uncharged amino acid residues of the −3/−1 cleavage site motifs conserved in all Cx isotypes at the indicated sites are marked in *bold* type.

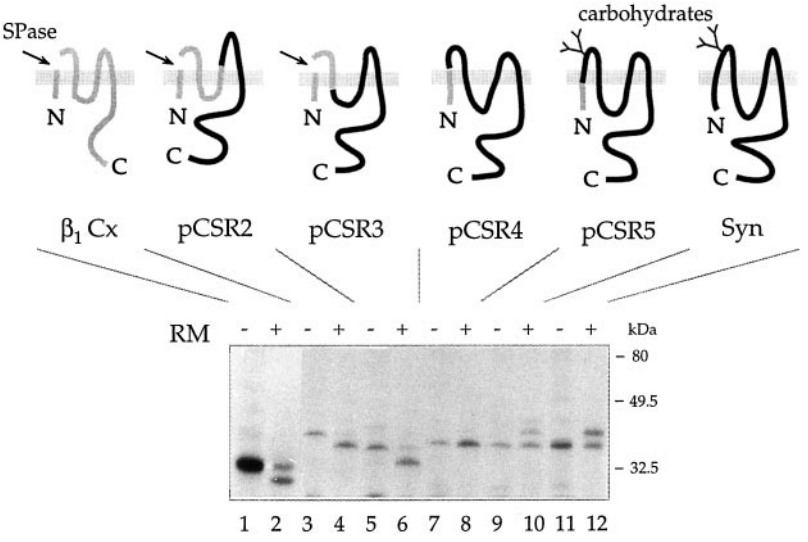

FIG. 6. **Translocation of chimeric β_1 Cx/Syn fusion proteins.** β_1 Cx/Syn chimeras (pCSR2-pCSR5), wt β_1 Cx, and wt Syn were translated in reticulocyte lysates in the presence of microsomes (+), and translation products were analyzed for SPase cleavage and *N*-glycosylation by SDS-PAGE and autoradiography. In control, translation products obtained in the absence of microsomes (−) were analyzed to indicate the electrophoretic mobility of non-glycosylated, full-length polypeptides. In the chimeras the Cx sequence (shown in *gray* in the topology schemes) was progressively replaced from the COOH terminus by Syn sequence (shown in *black*). While wt β_1 Cx and chimeras pCSR2 and 3 were cleaved (*lanes 2, 4,* and *6*), pCSR4, pCSR5, and wt Syn were not cleaved (*lanes 8, 10,* and *12*). Further replacement of TM1 resulted in addition in the *N*-glycosylation of pCSR5 (*lane 10*), as in wt Syn (*lane 12*).

second TM domain (TM2) and the first extracellular domain (E1) by Syn sequence abolished the cleavage completely (pCSR4; Fig. 6, *lane 8*). Also, no cleavage was observed for the chimera pCSR5 that consisted entirely of Syn sequence except its NH_2-terminal domain (Fig. 6, *lane 10*), and in the wt Syn protein (Fig. 6, *lane 12*). *N*-Glycosylation of the Syn authentic glycosylation sequence located within its first lumenal loop (22) occurred in wt Syn (Fig. 6, *lane 12*), and in the chimera pCSR5 (Fig. 5, *lane 10*) that both contain the first TM domain of Syn. However, glycosylation did not occur in the chimera pCSR4 (Fig. 5, *lane 8*) that also encodes the Syn authentic glycosylation sequence, but instead contains the first TM domain of the β_1 Cx. Taken together the results indicated that both, the TM1 and E1 domain, play an essential role for the access of SPase to the cleavage sites in the wt Cxs.

Increasing the Hydrophobic Character of the First TM Domain (TM1) of Cxs Prevented Their Inappropriate Cleavage by SPase—The hydrophobic core region (h-region) of the TM1 domain of Cxs has a length of only 18 amino acid residues, and in addition, it is interrupted by an arginine (Arg) residue in its center that further reduces the hydrophobic character of this region (see Fig. 4*B*). To determine if the weak hydrophobic character of this domain might be responsible for the Cx cleavage, three β_1 Cx mutants were constructed in which the hydrophobicity of the TM1 domain was increased. In the mutant β_1R32L, the central Arg-32 residue was substituted with leucine (Leu). In the mutant β_1+3L, three additional Leu residues were introduced immediately adjacent to the central Arg-32 residue. In the mutant β_1R32L+3L, the central Arg-32 residue was replaced by leucine, and three additional Leu residues were introduced. Cleavage of the mutants β_1R32L, and β_1+3L was significantly reduced (Fig. 7, *lanes 4* and *6*) compared with the wt β_1 protein (Fig. 7, *lane 2*), and cleavage of the mutant β_1R32L+3L was completely abolished (Fig. 7, *lane 8*). Membrane insertion and correct transmembrane topology of the mutants was verified by their association with the microsomal membranes after pelleting the microsomes through sucrose cushions, and by their *N*-glycosylation after introducing *N*-glycosylation consensus sites into the extracellular loops E1 and E2 of the β_1R32L+3L mutant (not shown).

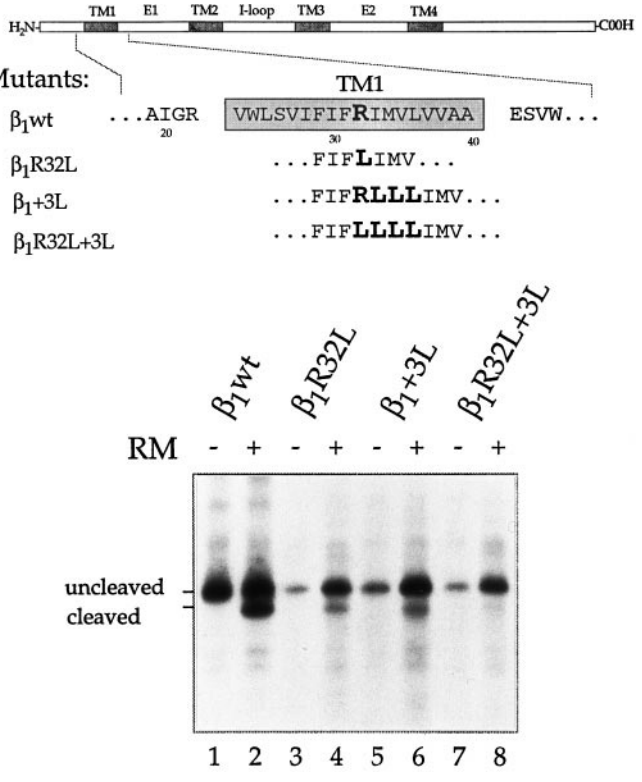

FIG. 7. **Influence of the hydrophobic character of the TM1 domain on SPase cleavage.** The hydrophobic character of the TM1 domain in β_1 Cx was increased by exchanging the central arginine (*R*) residue with leucine (*L*), and by introducing three additional leucine residues into the hydrophobic core region of the TM1 domain. Translation products obtained in the absence (−) and presence (+) of microsomes were analyzed by SDS-PAGE and visualized by autoradiography. In the mutants β_1R32L and β_1+3L, cleavage efficiency was drastically reduced (*lanes 4* and *6*) when compared with wt β_1 Cx (*lane 2*), and in the mutant β_1R32L+3L, cleavage was completely prevented (*lane 8*).

DISCUSSION

In this study we report that the synthesis of polytopic Cx membrane proteins in standard cell-free translation/translocation systems resulted in an aberrant proteolytic cleavage within their amino acid sequence that affected the entire pool of newly membrane integrated Cxs. These truncated Cxs differed from functional Cxs synthesized in tissues. This difference in Cx membrane integration *in vitro* and *in vivo* demonstrates that the membrane integration process of Cxs somehow differs from the membrane integration of other TM proteins.

The inability of the lysate system to generate normal, full-length membrane integrated Cx polypeptides was unexpected since this system has been found previously to accurately reproduce the biosynthesis of many other membrane proteins including several examples of structurally and functionally

related polytopic membrane proteins, such as ion channel subunits (28–31), aquaporins (32–34), and membrane pumps (35, 36). Subcellular Cx distribution studies (7, 37, 38) have indicated that Cxs follow the secretory pathway from the ER, to the Golgi and PM, suggesting that the ER-derived microsomal membranes used in the cell-free expression system as target membranes represent the appropriate intracellular membranes for Cx translocation. Also, the cleavage cannot be explained by arguing that the microsomes were derived from an inadequate source, since pancreatic acinar cells, from which the microsomes were prepared (18), synthesize endogenous Cx polypeptides (39, 40) and are able to integrate these proteins without aberrant cleavage into their ER membranes (7). Finally, *N*-glycosylation site tagging of α_1 and β_1 Cx (this study) combined with protease protection assays (7) demonstrated that the TM topology of Cxs integrated *in vitro* into microsomes corresponded to their natural TM topology with NH_2 and COOH termini correctly located outside the microsomal vesicles (in the cytoplasm) and the two extracellular loops located correctly inside the lumen of the microsomes. Therefore, an inappropriate membrane topology can also be excluded as a possibility that would lead to the Cx cleavage.

Amino acid sequencing of the cleaved Cxs identified cleavage sites at the COOH-terminal end of the TM1 domain, located in the border region between TM1 and the first extracellular loop (E1). Therefore, the NH_2-terminal domain and the TM1 domain was removed from the rest of the Cx polypeptide sequence by this cleavage. Analysis of the amino acid sequence adjacent to the cleavage sites showed that the sites had homology to known cleavage site motifs (small, uncharged amino acid residues in position −3 and −1 to the cleavage site) of SPase (12, 27). They were identified at the COOH-terminal ends of NH_2-terminal ER targeting SP sequences of secretory and transmembrane proteins (27) which are cleaved behind these motifs by this protease. Several such −3/−1 motifs are conserved in the Cx polypeptide isotypes in the border region between the TM1 and the E1 domains (compare Fig. 4*B*).

Analysis of the cleavage reaction further indicated that the cleavage was indeed performed by SPase. SPase is known to be present and active in microsomes (41). In Falk *et al.* (7) we reported that the cleavage occurred concomitant with the Cx polypeptide membrane integration, was strictly dependent on active, signal recognition particle-mediated protein translocation, and was restricted to the microsomal lumen. Here we report that the translocation of Cx/synaptophysin chimeras indicated that the TM1 domain and/or the first extracellular loop (E1) of the Cx sequence contained the cleavage signal and were essential for the cleavage reaction. Pretreatment of the microsomes with NEM, an alkylating agent that has been shown previously to prevent nascent chain translocation (23) indicated that insertion of the Cx polypeptides into the membrane was required for cleavage. Targeting and binding to the membrane bilayer was not sufficient. Depletion of the microsomes of their lumenal proteins had little effect on the cleavage reaction, suggesting that the cleavage was performed by a membrane-bound ER protease. Finally, several class-specific protease inhibitors had no effect on the cleavage reaction, even under conditions where direct access of the inhibitors to the lumen of the microsomes was ensured. SPase, in contrast to other known ER lumenal proteases is not affected by known protease inhibitors, a property attributed to its unusual cleavage mechanism (42). All these properties are indicative of a cleavage by SPase falsely performed on the Cx polypeptide sequence by this enzyme *in vitro*. Inappropriate uncovering and processing of "cryptic" SPase cleavage sites has been reported previously for some membrane proteins after modifying the amino acid sequence in or near the hydrophobic core region of their signal sequences (43–46). However, no inappropriate processing of a wt protein, as in the case of the Cxs, has been reported. Why then is the lysate system not able to generate full-length membrane integrated Cx polypeptides, and SPase efficiently recognizes and cleaves the Cx polypeptides within their functional sequence when they are translocated *in vitro*?

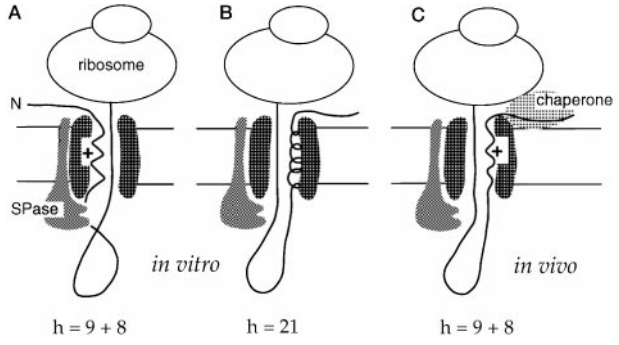

FIG. 8. **Schematic representation of the proposed locations of wt and elongated Cx TM1 domains in the ER translocon during Cx polypeptide translocation *in vitro* and *in vivo*.** *A,* during *in vitro* translation SPase has access to the cleavage site in the Cx sequence due to the short, relatively weak hydrophobic character of the Cx TM1 core region that leads to its mis-positioning as a cleavable SP. *B,* increasing the length of the hydrophobic region results in correct recognition and positioning of the TM1 domain as an internal SA sequence and SPase access is prevented. *C, in vivo*, an unknown factor, such as a chaperone, may bind to the Cx sequence and assist achieving the correct positioning of the TM1 domain in the translocon. SPase has no access to the cleavage site.

In the Cxs, the TM1 domain functions as an internal SA sequence,[2] suggesting that the cleavage could be due to an incorrect recognition of this domain as a cleavable SP sequence. Sequence comparison indicated a principal structural similarity between cleavable SP sequences and internal SA sequences. Both sequences consist of a short, positively charged NH_2-terminal region (n-region), a central hydrophobic core region (h-region), and a more polar COOH-terminal region (c-region) (47, 48); and many SA sequences of membrane proteins are followed by one or more −3/−1 cleavage site motifs, although they are not processed in detectable amounts by SPase *in vitro* or *in vivo*. However, an obvious difference between SP and SA sequences is the considerably longer h-region of the latter. While h-regions of cleaved SP sequences are typically 7–15 residues long and are rarely longer than 17 residues, the h-regions of uncleaved SA sequences range from 20 to 30 residues in length (48, 49). Nilsson *et al*. (48) found that the length of the h-region is directly decisive for its recognition as a SP or SA sequence. The different length results in a different positioning of SP and SA sequences within the translocon during the translocation process, allowing SPase to access and cleave NH_2-terminal SP sequences, while the cleavage of internal SA sequences is prevented. A sequence of 17–19 hydrophobic residues was determined as the critical length (48). In Cxs the hydrophobic core of the TM1 domain has a length of only 18 residues. In addition, it contains an arginine residue in its center that interrupts the hydrophobic character of this domain (see Fig. 4*B*).

To test the hypothesis that the relatively weak hydrophobic character of the Cx TM1 domain may cause its false recognition and positioning, β_1 Cx mutants with an increased hydrophobic character of their TM1 domain were generated. Replacing the central arginine residue with leucine, or elongating the h-region by 3 leucine residues to 21 residues already drastically

[2] M. Falk, unpublished data.

reduced the cleavage efficiency. Increasing the hydrophobicity further by replacing the central arginine, and in addition, elongating the h-region by 3 leucine residues into a homogenous stretch of 21 hydrophobic residues completely abolished the cleavage (Fig. 7). These results indicate that the SA sequence of wt Cxs is inappropriately recognized and positioned as a cleavable SP sequence when translated *in vitro*, due to its relatively weak hydrophobic character. The inappropriate cleavage can be overcome by increasing the hydrophobic character and the length of this domain (represented schematically in Fig. 8, *A* and *B*).

These findings, however, do not explain why the SA sequence of Cxs was not appropriately recognized *in vitro*. A mechanism that would explain this phenomenon is that a specific factor, such as a chaperone that normally is involved in the membrane integration of Cxs and, for example, binds to the Cx polypeptide sequence to aid in their correct positioning within the ER translocon (represented schematically in Fig. 8*C*), is absent or not functional in the cell-free expression system. This hypothesis is supported by our findings obtained with the expression of Cxs in transfected tissue culture cells (7). Overexpression of Cxs in different cell types resulted in the cleavage of a portion of the newly synthesized Cx polypeptides upon their translocation into the ER membranes that correlated with the expression level. This result suggests that a factor involved in their proper membrane integration has only a limited availability within the cell. Further experimentation will be aimed at the determination of the components that provide an appropriate positioning of the Cx polypeptides in the translocon to facilitate the synthesis of full-length membrane integrated Cxs *in vivo*.

Acknowledgments—We thank Nalin Kumar, Richard Scheller, Dieter Zopf, Peter Walter, and Rudolph Leube for generously providing cDNA clones and connexin chimeras, Lisa Bibbs and The Scripps Research Institute's Core Facility for protein sequencing, Angelika Kehlenbach and Jutta Falk-Marzillier for critically reading the manuscript, Jialing Lin and members of the Gilula laboratory for helpful discussions.

REFERENCES

1. Blobel, G., and Dobberstein, B. (1975) *J. Cell Biol.* **67,** 852–862
2. Rapoport, T. A., Jungnickel, B., and Kutay, U. (1996) *Annu. Rev. Biochem.* **65,** 271–303
3. High, S., and Laird, V. (1997) *Trends Cell Biol.* **7,** 206–210
4. Johnson, A. E. (1997) *Trends Cell Biol.* **7,** 90–95
5. Borel, A. C., and Simon, S. M. (1996) *Biochemistry* **35,** 10587–10594
6. Mothes, W., Heinrich, S. U., Graf, R., Nilsson, I. M., von Heijne, G., Brunner, J., and Rapoport, T. A. (1997) *Cell* **89,** 523–533
7. Falk, M. M., Kumar, N. M., and Gilula, N. B. (1994) *J. Cell Biol.* **127,** 343–355
8. Bruzzone, R., White, T. W., and Goodenough, D. A. (1996) *BioEssays* **18,** 709–718
9. Kumar, N. M., and Gilula, N. M. (1996) *Cell* **84,** 381–388
10. Nicholson, B., Dermietzel, R., Teplow, D., Traub, O., Willecke, K., and Revel, J.-P. (1987) *Nature* **329,** 732–734
11. Zimmer, D. B., Green, C. R., Evans, W. H., and Gilula, N. B. (1987) *J. Biol. Chem.* **262,** 7751–7763
12. Lively, M. O., and Walsh, K. A. (1983) *J. Biol. Chem.* **258,** 9488–9495
13. Krieg, P. A., and Melton, D. A. (1984) *Nucleic Acids Res.* **12,** 7057–7070
14. Falk, M. M., Sobrino, F., and Beck, E. (1992) *J. Virol.* **66,** 2251–2260
15. Hart, G. W., Brew, K., Grant, G. A., Bradshaw, R. A., and Lennarz, W. J. (1978) *J. Biol. Chem.* **254,** 9747–9753
16. Leube, R. E. (1995) *J. Cell Sci.* **108,** 883–894
17. Falk, M. M., Buehler, L. K., Kumar, N. M., and Gilula, N. B. (1997) *EMBO J.* **16,** 2703–2716
18. Walter, P., and Blobel, G. (1983) *Methods Enzymol.* **96,** 84–93
19. Nicchitta, C. V., and Blobel, G. (1993) *Cell* **73,** 989–998
20. Lingappa, V. R., Devillers-Thiery, A., and Blobel, G. (1977) *Proc. Natl. Acad. Sci. U. S. A.* **74,** 2432–2436
21. Anderson, D. J., Mostow, K. E., and Blobel, G. (1983) *Proc. Natl. Acad. Sci. U. S. A.* **80,** 7249–7253
22. Cowan, D., Linial, M., and Scheller, R. H. (1990) *Brain Res.* **509,** 1–7
23. Nicchitta, C. V., and Blobel, G. (1989) *J. Cell Biol.* **108,** 789–795
24. Bonifacino, J. S., and Lippincott-Schwartz, J. (1991) *Curr. Opin. Cell Biol.* **3,** 592–600
25. Hammond, C., and Helenius, A. (1995) *Curr. Opin. Cell Biol.* **7,** 523–529
26. Kopito, R. R. (1997) *Cell* **88,** 427–430
27. von Heijne, G. (1984) *J. Mol. Biol.* **173,** 243–251
28. Chavez, R. A., and Hall, Z. W. (1992) *J. Cell Biol.* **116,** 385–393
29. Rosenberg, R. L., and East, J. E. (1992) *Nature* **360,** 166–169
30. Shen, N. V., Chen, X., Boyer, M. M., and Pfaffinger, P. J. (1993) *Neuron* **11,** 67–77
31. Shtrom, S. S., and Hall, Z. W. (1996) *J. Biol. Chem.* **271,** 25506–25514
32. Conroy, W. G., Vernallis, A. B., and Berg, D. K. (1992) *Neuron* **9,** 679–691
33. Shi, L.-B., Skach, W. R., Ma, T., and Verkman, A. S. (1995) *Biochemistry* **34,** 8250–8256
34. Bai, L., Fushimi, F., Sasaki, S., and Marumo, F. (1996) *J. Biol. Chem.* **271,** 5171–5176
35. Bamberg, K., and Sachs, G. (1994) *J. Biol. Chem.* **269,** 16909–16919
36. Jaunin, P., Jaisser, R., Beggah, A. T., Takeyasu, K., Mangeat, P., Rossier, B. C., Horisberger, J.-D., and Geering, K. (1993) *J. Cell Biol.* **123,** 1751–1759
37. Musil, L. S., and Goodenough, D. A. (1991) *J. Cell Biol.* **115,** 1357–1374
38. Laird, D. W., Castillo, M., and Kasprzak, L. (1995) *J. Cell Biol.* **131,** 1193–1203
39. Dermietzel, D., Leibstein, A., Frixen, U., Jannsen-Timmen, U., Traub, O., and Willecke, K. (1984) *EMBO J.* **3,** 2261–2270
40. Hertzberg, E. L., and Skibbens, R. B. (1984) *Cell* **39,** 61–69
41. Evans, E. A., Gilmore, R., and Blobel, G. (1986) *Proc. Natl. Acad. Sci. U. S. A.* **83,** 581–585
42. Dalbey, R. E., and von Heijne, G. (1992) *Trends Biochem Sci.* **17,** 474–478
43. Lipp, J., and Dobberstein, B. (1986) *Cell* **46,** 1103–1112
44. Schmid, S., and Spiess, M. (1988) *J. Biol. Chem.* **263,** 16886–16891
45. Hegner, M., von Kieckebusch-Gück, A., Falchetto, R., James, P., Semenza, G., and Mantei, N. (1992) *J. Biol. Chem.* **267,** 16928–16933
46. Roy, P., Chatellard, C., Lemay, G., Crine, P., and Boileau, G. (1993) *J. Biol. Chem.* **268,** 2699–2704
47. Nilsson, I., and von Heijne, G. (1991) *J. Biol. Chem.* **266,** 3408–3410
48. Nilsson, I. M., Whitley, P., and von Heijne, G. (1994) *J. Cell Biol.* **126,** 1127–1132
49. von Heijne, G. (1986) *J. Mol. Biol.* **189,** 239–242